ENHANCED CAPABILITIES OF THE NASA LANGLEY THERMAL ACOUSTIC FATIGUE APPARATUS

Stephen A. Rizzi and Travis L. Turner
Structural Acoustics Branch
NASA Langley Research Center
Hampton, VA 23681-0001

ABSTRACT

This paper presents newly enhanced acoustic capabilities of the Thermal Acoustic Fatigue Apparatus at the NASA Langley Research Center. The facility is a progressive wave tube used for sonic fatigue testing of aerospace structures. Acoustic measurements for each of the six facility configurations are shown and comparisons with projected performance are made.

INTRODUCTION

The design of supersonic and hypersonic vehicle structures presents a significant challenge to the airframe analyst because of the wide variety and severity of environmental conditions. One of the more demanding of these is the high intensity noise produced by the propulsion system and turbulent boundary layer [1]. Complicating effects include aero-thermal loads due to boundary layer and local shock interactions, static mechanical preloads, and panel flutter. Because of the difficulty in accurately predicting the dynamic response and fatigue of structures subject to these conditions, experimental testing is often the only means of design validation. One of the more common means of simulating the thermal-vibro-acoustic environment is through the use of a progressive wave tube. The progressive wave tube facility at NASA Langley Research Center, known as the Thermal Acoustic Fatigue Apparatus (TAFA), has been used in the past to support development of the thermal protection system for the Space Shuttle and National Aerospace Plane [2]. It is presently being used for sonic fatigue studies of the wing strake subcomponents on the High Speed Civil Transport [3].

The capabilities of the TAFA were previously documented by Clevenson and Daniels [4]. The system was driven by two Wyle WAS 3000 airstream modulators which provided an overall sound pressure level range of between 125 and 165 dB and a useful frequency range of 50-200 Hz. A 360 kW quartz lamp bank provided radiant heat with a peak heat flux of 54 W/cm^2. A schematic of the facility is shown in Figure 1. Representative spectra and coherence plots are shown in Figures 2 and 3. Since that time, the facility has undergone significant enhancements designed to improve its acoustic capabilities; the heating capabilities were not changed. The objectives of the enhancements were to increase the maximum overall sound pressure level (OASPL) to 178 dB, increase the frequency bandwidth to 500 Hz and improve the uniformity of the sound pressure field in the test section. This paper

Published in *Proceedings of the 6th International Conference on Recent Advances in Structural Dynamics*, Vol. II, Ed. Ferguson, Wolfe, Mei, 1997, pp. 919 – 933.

documents the new capabilities of the TAFA and makes comparisons with the projected performance.

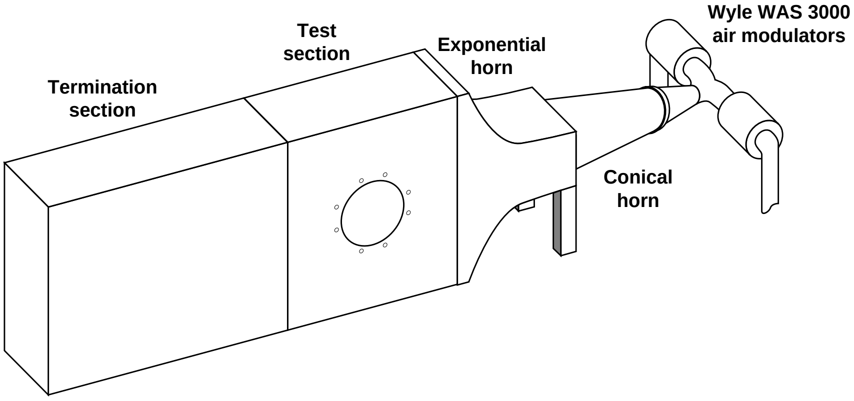

Figure 1: Schematic of the old TAFA facility.

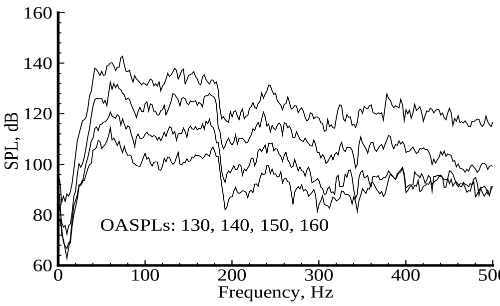

Figure 2: Test section spectra of the old TAFA facility.

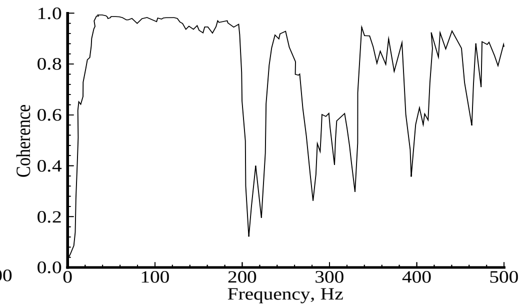

Figure 3: Test section coherence of the old TAFA facility.

FACILITY DESCRIPTION

In order to meet the design objectives, extensive modifications were made to the sound generation system and to the wave tube itself. A theoretical increase of 6 dB OASPL was projected by designing the system to utilize eight WAS 3000 air modulators compared to the two used in the previous system. A further increase of nearly 5 dB was expected by designing the test section to accommodate removable water-cooled insert channels which reduced its cross-sectional area from 1.9m x 0.33m to 0.66m x 0.33m. The frequency range was increased through the use of a longer horn design with a lower (15 Hz vs. 27 Hz in the old facility) cut-off frequency, use of insert channels in the test section to shift the frequency of significant standing waves above 500 Hz, and design of facility sidewall structures with resonances above 1000 Hz. The uniformity of the sound pressure field in the test section was improved through several means. A new, smooth exponential horn was designed to avoid the impedance mismatches of the old design. To minimize the effect of uncorrelated, broadband noise (which develops as a byproduct of the sound generation system), a unique design was adopted which allows for the use of

Published in *Proceedings of the 6th International Conference on Recent Advances in Structural Dynamics*, Vol. II, Ed. Ferguson, Wolfe, Mei, 1997, pp. 919 – 933.

either two-, four-, or eight-modulators. When testing at the lower excitation levels for example, a two-modulator configuration might be used to achieve a lower background level over that of the four- or eight-modulator configurations. In doing so, the dynamic range is extended. Lastly, a catenoidal design for the termination section was used to smoothly expand from the test section.

Schematics of the facility in the three full test section configurations are shown in Figures 4-6. In the two-modulator configuration, the 2 x 4 transition cart acts to block all but two of the eight modulators. The facility is converted from the two- to four-modulator configuration by the removal of the 2 x 4 transition cart and connection of two additional modulators. In doing so, the modulator transition cart slides forward and thereby maintains the continuous exponential expansion of the duct. In the four-modulator configuration, the 4 x 8 transition cart acts to block the two upper and two lower modulators. Removal of this component and connection of the four additional modulators converts the facility to the eight-modulator configuration. Again, the continuous exponential expansion is maintained as the modulator transition cart slides forward.

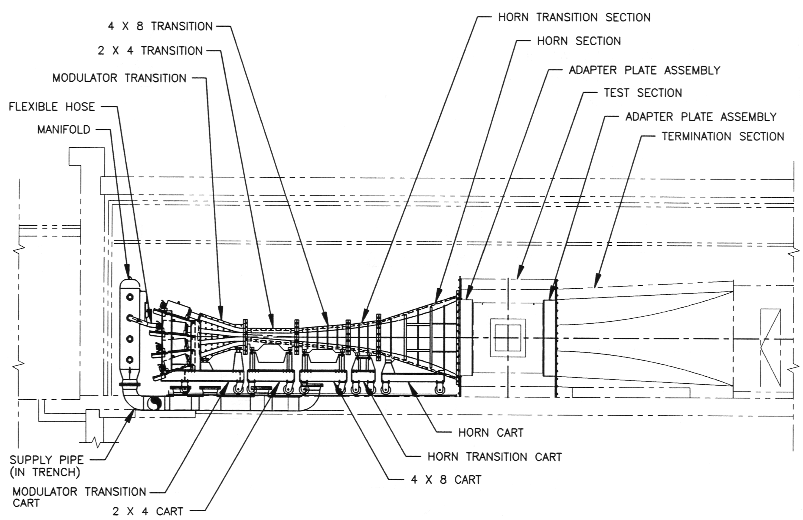

Figure 4: Two-modulator full test section configuration.

Published in *Proceedings of the 6th International Conference on Recent Advances in Structural Dynamics*, Vol. II, Ed. Ferguson, Wolfe, Mei, 1997, pp. 919 – 933.

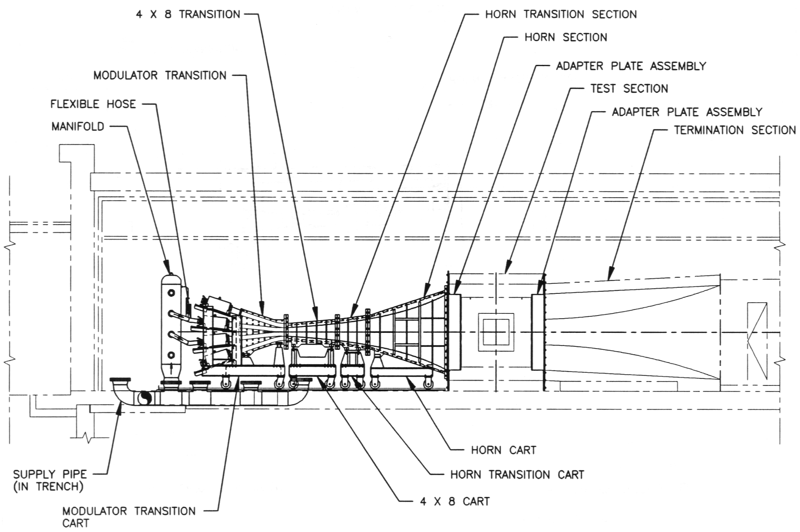

Figure 5: Four-modulator full test section configuration.

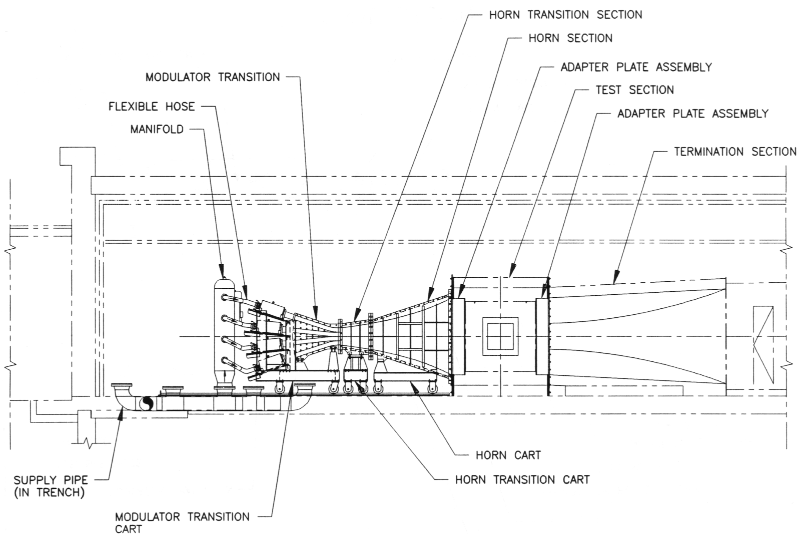

Figure 6: Eight-modulator full test section configuration.

Schematics of the three reduced test section configurations are shown in Figures 7-9. In these configurations, the horn cart is discarded and the horn transition cart mates directly to the test section. Water-cooled inserts are used in the test section to reduce its cross-sectional area. Upper and lower inserts in the termination section are used to smoothly transition the duct area to the full dimension at the exit. Conversion from the two- to the four-modular configuration and from the four- to the eight-modulator configuration is again accomplished through removal of the 2 x 4 and 4 x 8 transition carts, respectively.

Published in *Proceedings of the 6th International Conference on Recent Advances in Structural Dynamics*, Vol. II, Ed. Ferguson, Wolfe, Mei, 1997, pp. 919 – 933.

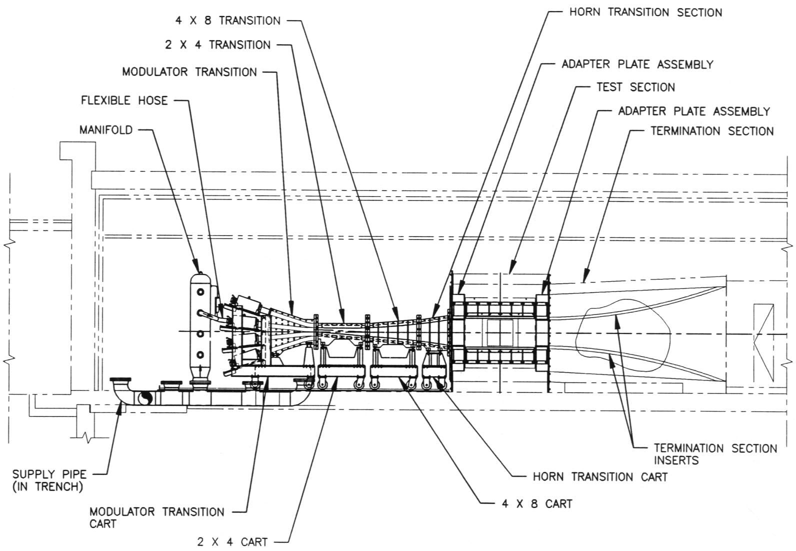

Figure 7: Two-modulator reduced test section configuration.

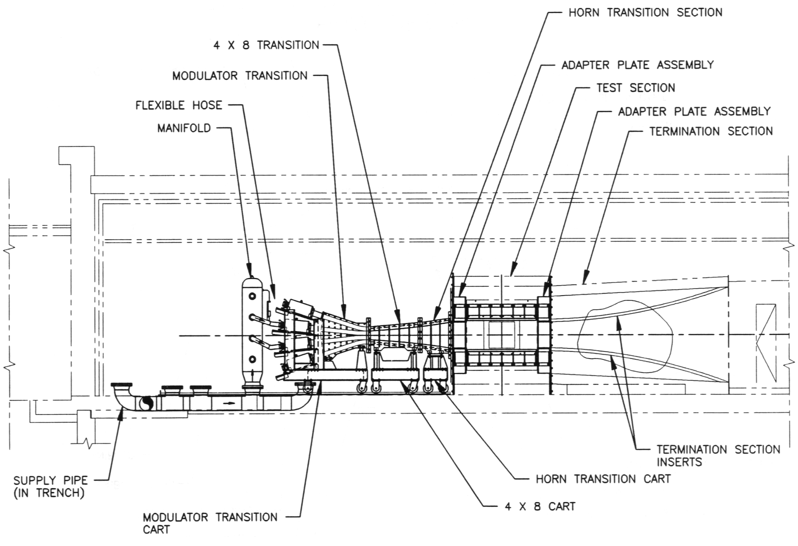

Figure 8: Four-modulator reduced test section configuration.

TEST PROCEDURE

Measurements were taken for several conditions in each of the six facility configurations. Each modulator was supplied with air at a pressure of 207 kPa (mass flow rate of approximately 8.4 kg/s) and was electrically driven with the same broadband (40-500 Hz) signal. Acoustic pressures were measured at several locations along the length of the progressive wave tube using B&K model 4136 microphones and Kulite model MIC-190-HT pressure transducers, see Table 1. The positive x-direction is defined in the two-modulator full configuration (from the modulator exit) along the direction of the duct. The positive y-direction is taken vertically from the horizontal centerline of the

Published in *Proceedings of the 6th International Conference on Recent Advances in Structural Dynamics*, Vol. II, Ed. Ferguson, Wolfe, Mei, 1997, pp. 919 – 933.

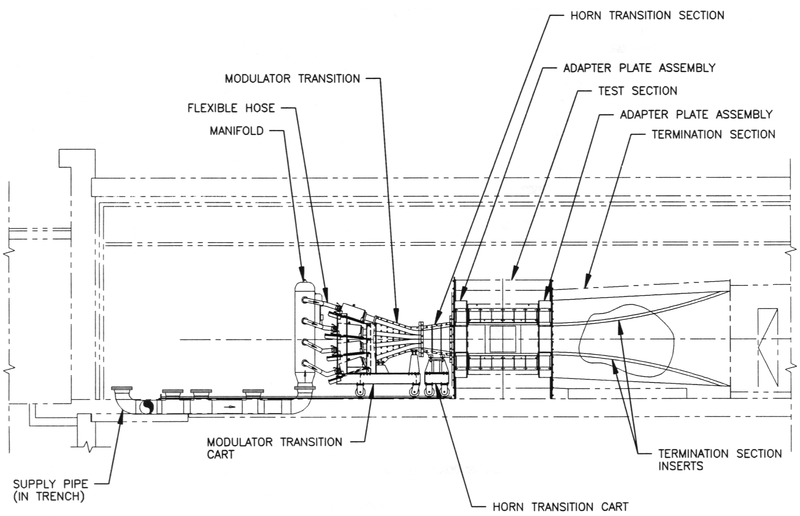

Figure 9: Eight-modulator reduced test section configuration.

duct and the positive z-direction is defined from the left sidewall of the duct as one looks downstream.

Table 1: Kulite (K) and microphone (M) locations of acoustic measurements.

Loc.	Description	Type	Coordinate (m)
1	Test Sect. Horizontal Centerline Upstream	K	7.75, 0, 0
2	Test Sect. Horizontal Centerline Downstream	K	8.71, 0, 0
5	Test Sect. Vertical Centerline Top	M	8.23, 0.3, 0
15	Test Sect. Horizontal/Vertical Centerline	K	8.23, 0, 0
25	Test Sect. Vertical Centerline Bottom	M	8.23, -0.3, 0
28	2x4 Horizontal/Vertical Centerline	M	2.19, 0, 0
29	4x8 Horizontal Centerline, ¾ Downstream	M	3.66, 0, 0
30	Horn Tran, Hor. Centerline, ¾ Downstream	M	4.75, 0, 0
35	Termination Horizontal/Vertical Centerline	M	12.46, 0, 0.17

The acoustic pressure at location 1 was used as a reference measurement for shaping the input spectrum and for establishing the nominal overall sound pressure level for each test condition. For each configuration, the input spectrum to the air modulators was manually shaped through frequency equalization to produce a nearly flat spectrum at the reference pressure transducer. Data was acquired at the noise floor level (flow noise only) and at overall levels above the noise floor in 6 dB increments (as measured at the reference location) up to the maximum achievable. Thirty-two seconds of time data were collected at a sampling rate of 4096 samples/s for each transducer in each test condition. Post-processing of the time data was performed to generate averaged spectra and coherence functions with a 1-Hz frequency resolution.

RESULTS

For each facility configuration, plots of the following quantities are presented: normalized input spectrum to the air modulators, minimum to maximum sound pressure levels at the reference location, maximum sound pressure levels in the test section, maximum sound pressure levels upstream and downstream of the test section, and vertical and horizontal coherence in the test section. The minimum levels in each case correspond to the background noise produced by the airflow through the modulators.

Normalized input voltage spectra to each modulator for each configuration are shown in Figures 10, 15, 20, 25 and 30. These spectra were generated to achieve as flat an output spectrum as possible at the reference location for the frequency range of interest (40-200 Hz for the full section, 40-500 Hz for the reduced section). As expected, the significant difference between the full and reduced configurations is seen in the high (>200 Hz) frequency content.

Figure 11 shows a background noise level of 126 dB (the lowest of all configurations) for the two-modulator full test section configuration. Nearly flat spectra are observed below 210 Hz for levels above 130 dB, giving a dynamic range of about 32 dB. The flat spectrum shape is a significant improvement over the performance of the old configuration as shown in Figure 2. Standing waves are evident at frequencies of 210, 340 and 480 Hz. For this reason, the full section operation is limited to less than 210 Hz or to the 220-330 and 370-480 Hz frequency bands. The effect of standing waves are explored in further depth in the next section. The spectra in Figure 12 indicate a nearly uniform distribution in the x-direction throughout the test section. It is interesting to note that Figure 13 shows no sign of standing waves upstream of the test section, confirming that the cause is associated with the test section. Lastly, a near perfect coherence between upstream and downstream, and upper and lower test section locations is shown in Figure 14 for frequencies between 40 and 210 Hz. Again, this is a significant improvement over the performance of the old configuration (Figure 3).

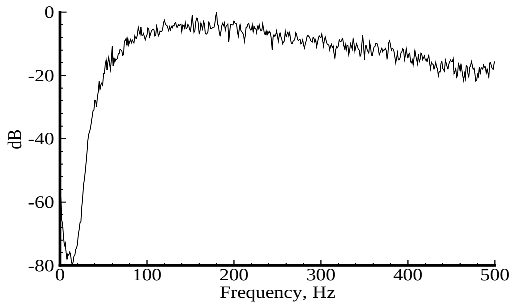

Figure 10: Normalized input spectrum (2-modulator full).

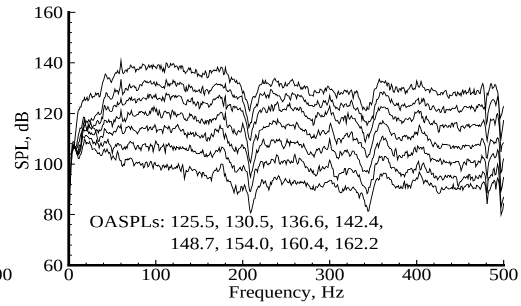

Figure 11: Min to max SPL at location 1 (2-modulator full).

Published in *Proceedings of the 6th International Conference on Recent Advances in Structural Dynamics*, Vol. II, Ed. Ferguson, Wolfe, Mei, 1997, pp. 919 – 933.

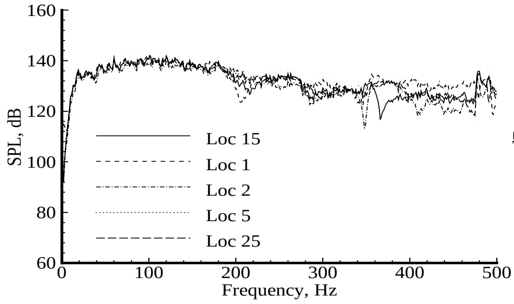

Figure 12: SPL in test section at max level (2-modulator full).

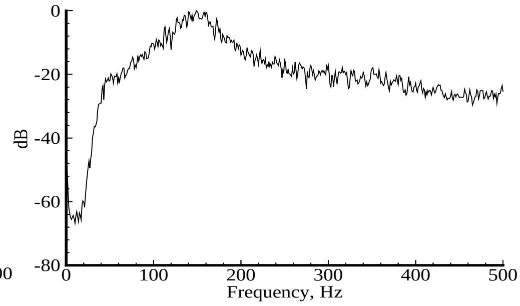

Figure 15: Normalized input spectrum (4-modulator full).

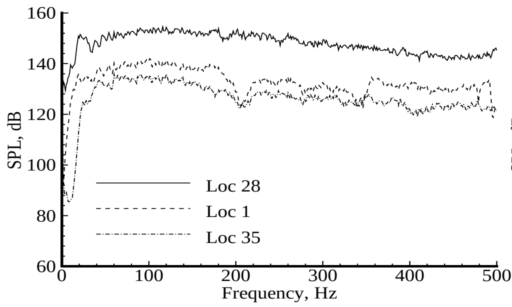

Figure 13: SPL along length of TAFA (2-modulator full).

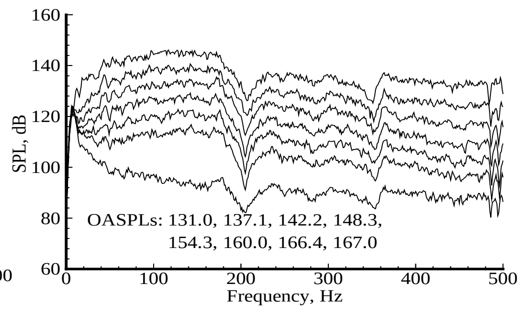

Figure 16: Min to max SPL at location 1 (4-modulator full).

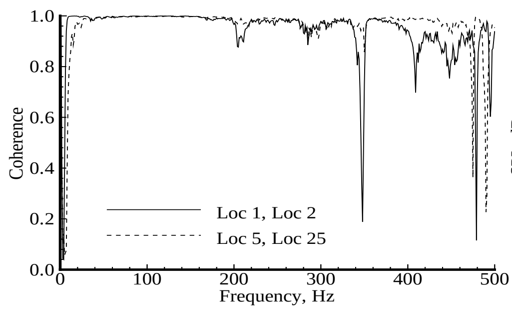

Figure 14: Test section coherence (2-modulator full).

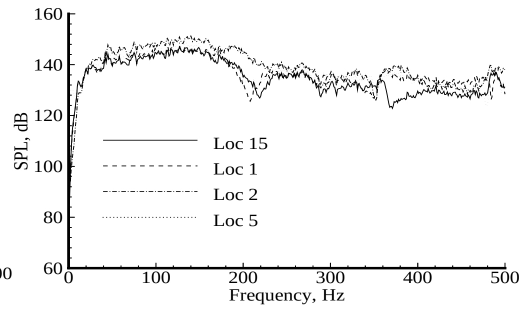

Figure 17: SPL in test section at max level (4-modulator full).

The four-modulator full configuration exhibits similar behavior as the two-modulator full configuration as seen in Figures 16-19. The lowest level at which a uniform spectrum is achieved is 137 dB, giving a dynamic range of roughly 30 dB in this configuration. Lastly, the eight-modulator full configuration results, shown in Figures 21-24, indicate a noise floor of about 142 dB and dynamic range of 22 dB.

Published in *Proceedings of the 6th International Conference on Recent Advances in Structural Dynamics*, Vol. II, Ed. Ferguson, Wolfe, Mei, 1997, pp. 919 – 933.

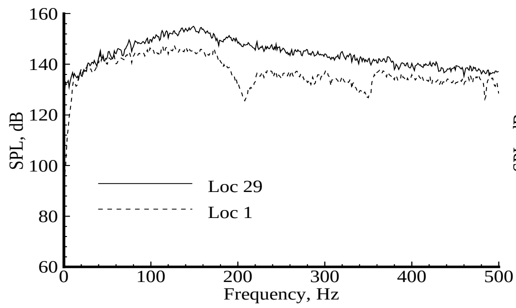

Figure 18: SPL along length of TAFA (4-modulator full).

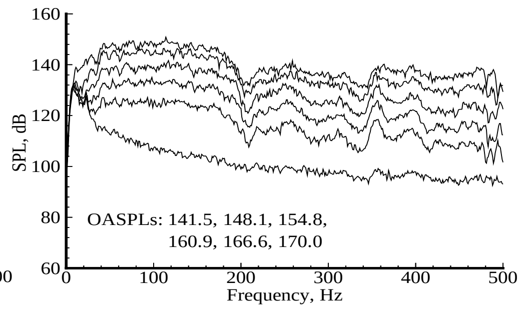

Figure 21: Min to max SPL at location 1 (8-modulator full).

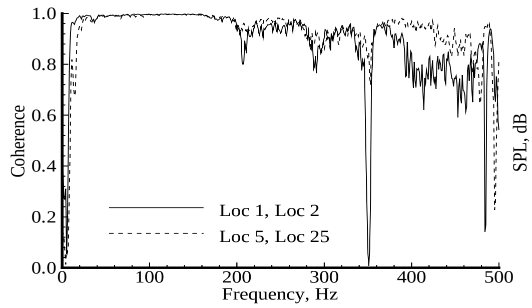

Figure 19: Test section coherence (4-modulator full).

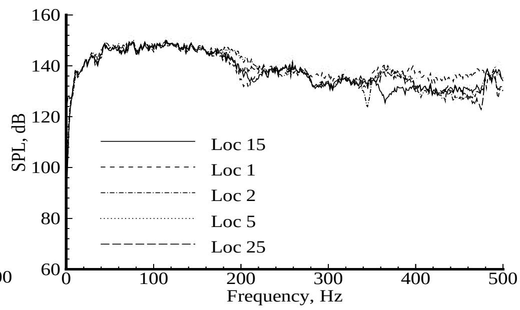

Figure 22: SPL in test section at max level (8-modulator full).

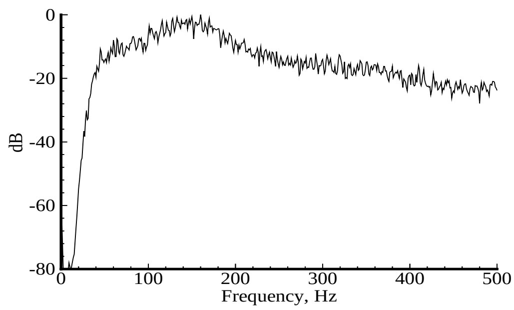

Figure 20: Normalized input spectrum (8-modulator full).

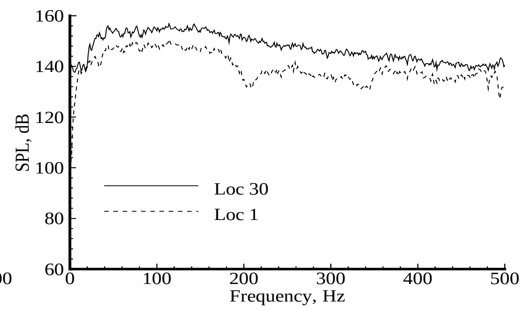

Figure 23: SPL along length of TAFA (8-modulator full).

Published in *Proceedings of the 6th International Conference on Recent Advances in Structural Dynamics*, Vol. II, Ed. Ferguson, Wolfe, Mei, 1997, pp. 919 – 933.

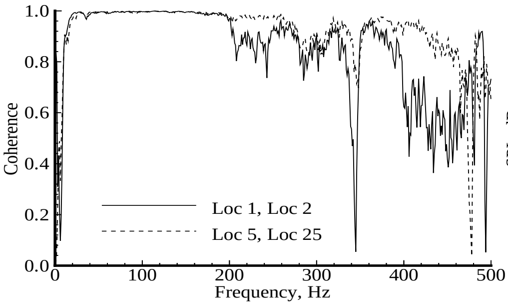

Figure 24: Test section coherence (8-modulator full).

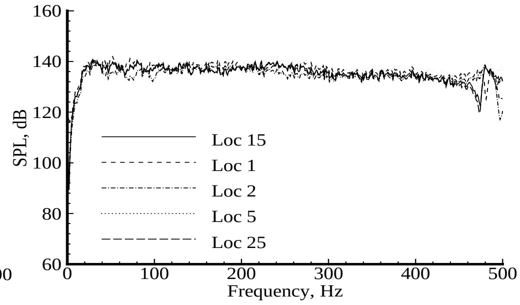

Figure 27: SPL in test section at max level (2-modulator reduced).

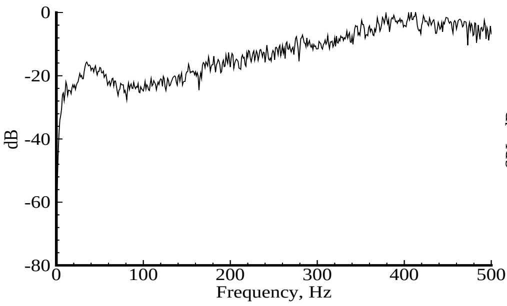

Figure 25: Normalized input spectrum (2-modulator reduced).

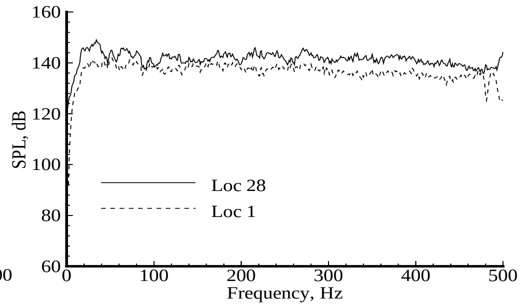

Figure 28: SPL along length of TAFA (2-modulator reduced).

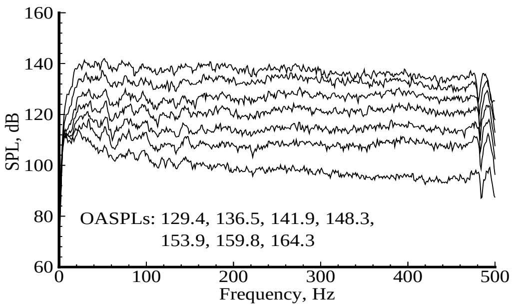

Figure 26: Min to max SPL at location 1 (2-modulator reduced).

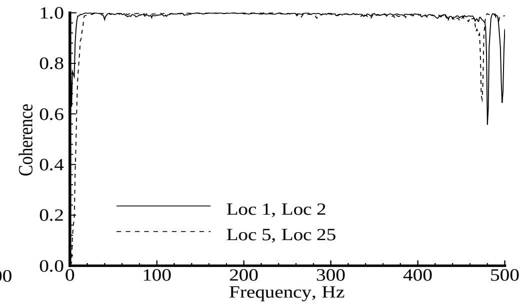

Figure 29: Test section coherence (2-modulator reduced).

The reduced test section configurations are used to increase the frequency range and maximum sound pressure level in the test section. Results for the two-modulator reduced configuration, shown in Figures 26-29, indicate a nearly flat spectrum between 40 and 480 Hz, a noise floor of 129 dB and a dynamic range of about 28 dB. Coherence in the test section is nearly unity over this frequency range. This represents a significant improvement over the old facility configuration. Results of similar quality indicate a dynamic range of roughly 26 and 29 dB for the four- (Figures 31-34) and eight-modulator (Figures 36-39) configurations, respectively. Note that the coherence for these

Published in *Proceedings of the 6th International Conference on Recent Advances in Structural Dynamics*, Vol. II, Ed. Ferguson, Wolfe, Mei, 1997, pp. 919 – 933.

configurations is slightly reduced at the high frequencies, but is still very good out to 480 Hz.

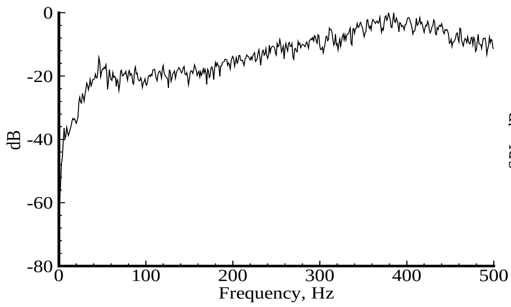

Figure 30: Normalized input spectrum (4-modulator reduced).

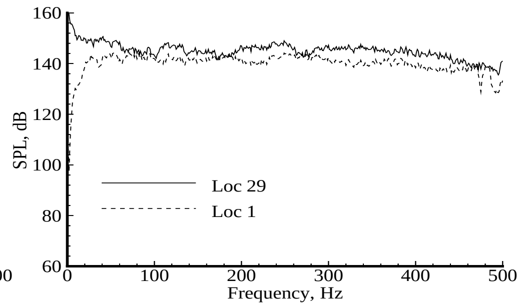

Figure 33: SPL along length of TAFA (4-modulator reduced).

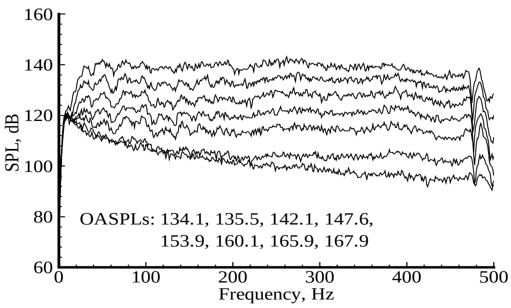

Figure 31: Min to max SPL at location 1 (4-modulator reduced).

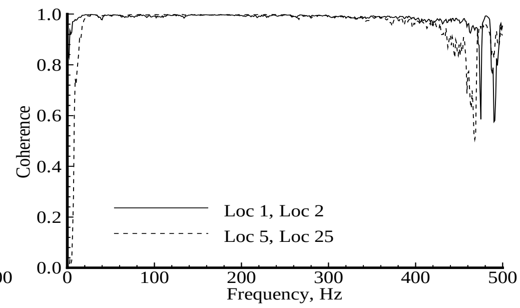

Figure 34: Test section coherence (4-modulator reduced).

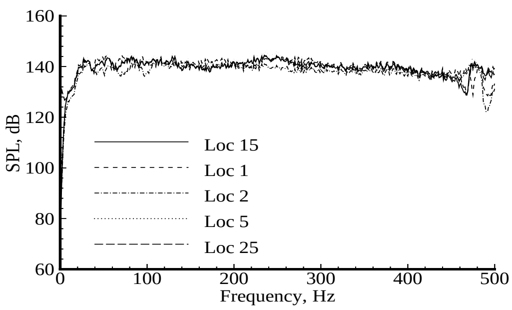

Figure 32: SPL in test section at max level (4-modulator reduced).

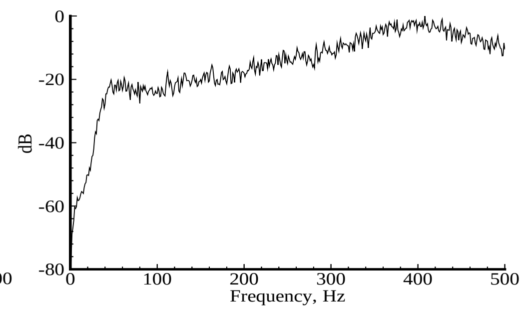

Figure 35: Normalized input spectrum (8-modulator reduced).

Published in *Proceedings of the 6th International Conference on Recent Advances in Structural Dynamics*, Vol. II, Ed. Ferguson, Wolfe, Mei, 1997, pp. 919 – 933.

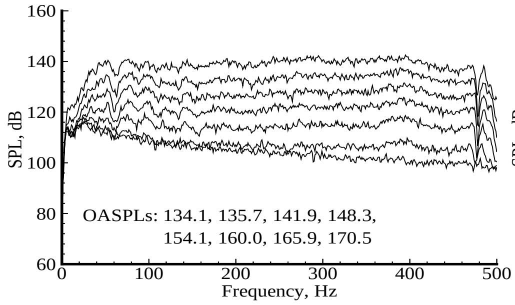

Figure 36: Min to max SPL at location 1 (8-modulator reduced).

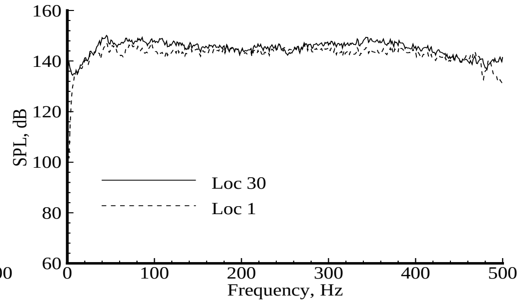

Figure 38: SPL along length of TAFA (8-modulator reduced).

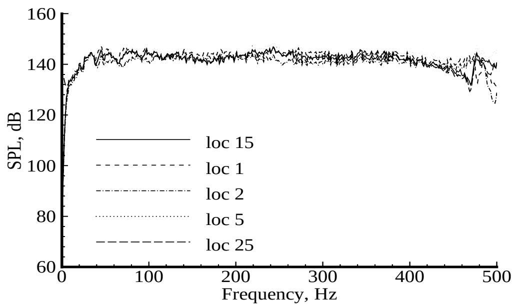

Figure 37: SPL in test section at max level (8-modulator reduced).

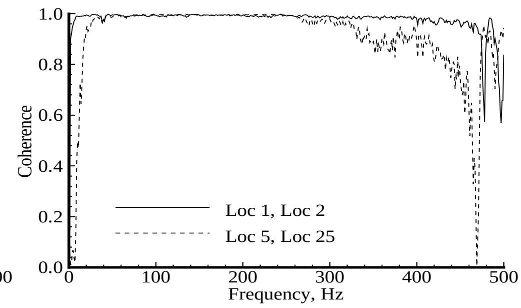

Figure 39: Test section coherence (8-modulator reduced).

Table 2 presents a summary of the maximum average OASPL for each facility configuration. In each case, the number of active modulators were run at maximum power as an independent group (independently for the single modulator case) and the results averaged. For example, results for one active modulator were obtained by running each modulator individually and averaging the resulting pressures.

Table 2: Summary of maximum average overall sound pressure levels (dB).

	Number of Active Modulators			
Configuration	1	2	4	8
2-Modulator Red.	160.4	164.3		
2-Modulator Full	156.7	162.2		
4-Modulator Red.	159.1	—	167.9	
4-Modulator Full	155.6	161.2	167.0	
8-Modulator Red.	158.4	—	—	171.7*
8-Modulator Full	153.0	158.4	164.5	170.0

*Pressure scaled by $^{8}/_{7}$ from 7-modulator run

Published in *Proceedings of the 6th International Conference on Recent Advances in Structural Dynamics*, Vol. II, Ed. Ferguson, Wolfe, Mei, 1997, pp. 919 – 933.

DISCUSSION

In this section, limiting behaviors of the full and reduced test section configurations are explored and the effect of test section inserts, modulator coupling and wave tube performance are discussed.

Limiting Behaviors

The auto-spectra from the full test section configurations exhibit sharp reductions in level at approximately 210, 340, and 480 Hz. This behavior corresponds to measurements near nodes of vertical (height) standing waves in the test section portion of the wave tube. Table 3 summarizes theoretical, resonant frequencies and corresponding modal indices of the test section duct resonances within the excitation bandwidth. The modal indices *m* and *n* correspond to half wavelengths in the vertical and transverse (width) directions of the cross section, respectively. There are several resonances that may be excited below 500 Hz, but only three of these appear to be significant at the test section transducer locations (about the horizontal centerline). Because of the presence of air flow in the facility and lack of measurements in the cross section, it is difficult to correlate the experimental and theoretical modes. Measurements of the acoustic pressure at several locations in a cross-section of the duct will be necessary to fully characterize the resonant behavior. It is sufficient to say that the usable frequency range in the full test section configurations is approximately 40-210 Hz near the horizontal centerline.

Acoustic pressure auto-spectra from the reduced test section configurations are essentially flat to almost 500 Hz. This is due to the fact that only two resonances are within the excitation bandwidth for this configuration, see Table 3. A sharp reduction is noted in the vicinity of 480 Hz. Although the (m=1, n=0) resonance does not appear to be significant, close inspection of the data (not shown) indicates its presence. Therefore, the usable frequency range for the reduced test section configurations is approximately 40-500 Hz.

Table 3: Theoretical resonant frequencies of test section duct modes in Hz.

Trans. Index (n)	Vertical Index (m) 0	1	2	3	4	5
	Full Test Section (1.9m x 0.33m)					
0	0.0	84.62	169.24	253.86	338.48	423.10
1	465.41	473.04	495.23	530.14		
	Reduced Test Section (0.66m x 0.33m)					
0	0.0	250.61	501.21			
1	465.41	528.59				

Published in *Proceedings of the 6th International Conference on Recent Advances in Structural Dynamics*, Vol. II, Ed. Ferguson, Wolfe, Mei, 1997, pp. 919 – 933.

Performance of Test Section Configurations

For constant input acoustic power, the change from full to reduced test section configurations should theoretically result in a 4.7 dB increase in OASPL. However, Table 2 shows that increases of only 2.1 (e.g. 164.3-162.2), 0.9, and 1.7 dB were realized for the two-, four- and eight-modulator configurations. The system efficiency (actual/expected mean-square pressure) of the two-, four- and eight-modulator reduced configurations is 38, 40 and 44 percent, respectively, compared with 51, 63 and 62 percent for the two-, four- and eight-modulator full configurations. The expected pressure is calculated based upon a input-scaled value of the rated acoustic power of the WAS 3000 modulator assuming incoherent sources (3 dB per doubling). In general, the full section efficiency is greater than the corresponding reduced section efficiency. While the reason for this phenomena is not known, it is conjectured that the lack of expansion in the reduced configurations limits the development of plane waves. Therefore, phase and amplitude mismatches between acoustic sources may be accentuated.

Modulator Coupling Performance

A simplified waveguide analysis for coherent, phase-matched sources predicts increases in OASPL as shown in Table 4. Measured performance gains were less than predicted because of the assumptions of the waveguide analysis (inactive source area treated as hard wall), and possible reductions due to phase differences between modulators and non-parallel wave fronts at the exit of the modulator cart, see Figures 4-9. The latter effect is due to different angles of inclination of the sources relative to the axis of the wave tube. The greater gains achieved in the full test section configurations support the above contention that they are more efficient than the reduced configurations in combining the acoustic sources.

Table 4: Change in SPL (dB) from 1 to max. number of active modulators.

Configuration	Δ SPL from 1 Active Mod. (Meas/Pred)
2-Modulator Red. (2 active mods.)	3.9 / 6.53
2-Modulator Full (2 active mods.)	5.5 / 6.53
4-Modulator Red. (4 active mods.)	8.8 / 13.98
4-Modulator Full (4 active mods.)	11.4 / 13.98
8-Modulator Red. (8 active mods.)	13.3 / 22.10
8-Modulator Full (8 active mods.)	17.0 / 22.10

Wave Tube Performance

A change in configuration from the two- to the four-modulator configurations, and from the four- to the eight-modulator configurations, will result in an incremental increase of 3 dB in OASPL if the individual sources are phase-matched. This is due to a pure doubling of the power without any change in the radiation impedance of the individual sources. For the reduced configurations, a 3.6 and 3.8 dB increase are observed, respectively. A 4.8 and

3.0 dB increase are observed for the full configurations, respectively. Note that a greater than 3 dB increase is possible when the higher modulator configuration (for example, the four-modulator reduced configuration) is less susceptible than the lower modulator configuration (the two-modulator reduced configuration) to phase mismatches between modulators. This seems plausible because any such mismatches are averaged over a larger number of sources.

SUMMARY

Modifications to the NASA Langley TAFA facility resulted in significant improvements in the quality and magnitude of the acoustic excitation over the previous facility. The maximum OASPL was increased by over 6 dB (vs the previous 165 dB) with a nearly flat spectrum between 40-210 and 40-480 Hz for the full and reduced test section configurations, respectively. In addition, the coherence over the test section was excellent. These improvements, however, did not meet the objective for a maximum OASPL of 178 dB.

There are several reasons why the maximum OASPL did not meet the objectives, including a lack of expansion in the reduced configurations and phase differences between modulators. A detailed computational analysis would be desirable to indicate the source of the inefficiencies and to help identify possible means of increasing the overall system performance.

ACKNOWLEDGEMENTS

The authors wish to thank Mr. H. Stanley Hogge and Mr. George A. Parker for their support in configuring and running the facility. We wish to also thank Mr. James D. Johnston, Jr. of NASA Johnson Space Center for loan of four Wyle air modulators.

REFERENCES

1. Maestrello, L., Radiation from a Panel Response to a Supersonic Turbulent Boundary Layer, *Journal of Sound and Vibration,* 1969, **10**(2), pp. 261-295.
2. Pozefsky, P., Blevins, R.D., and Langanelli, A.L., Thermal-Vibro-Acoustic Loads and Fatigue of Hypersonic Flight Vehicle Structure, AFWAL-TR-89-3014,
3. Williams, L.J., HSCT Research Gathers Speed, *Aerospace America*, April 1995, pp. 32-37.
4. Clevenson, S.A. and Daniels, E.F., Capabilities of the Thermal Acoustic Fatigue Apparatus, NASA TM 104106, February 1992.

Published in *Proceedings of the 6th International Conference on Recent Advances in Structural Dynamics*, Vol. II, Ed. Ferguson, Wolfe, Mei, 1997, pp. 919 – 933.